THE JOURNAL OF PHYSICAL CHEMISTRY B

Article

pubs.acs.org/JPCB

Theoretical Study of the Protonation of the One-Electron-Reduced Guanine–Cytosine Base Pair by Water

Sodio C. N. Hsu, Tzu-Pin Wang, Chai-Lin Kao, Hui-Fen Chen, Po-Yu Yang, and Hsing-Yin Chen*

Department of Medicinal and Applied Chemistry, Kaohsiung Medical University, Kaohsiung 807, Taiwan

Supporting Information

ABSTRACT: Prototropic equilibria in ionized DNA play an important role in charge transport and radiation damage of DNA and, therefore, continue to attract considerable attention. Although it is well-established that electron attachment will induce an interbase proton transfer from N1 of guanine (G) to N3 of cytosine (C), the question of whether the surrounding water in the major and minor grooves can protonate the one-electron-reduced G:C base pair still remains open. In this work, density functional theory (DFT) calculations were employed to investigate the energetics and mechanism for the protonation of the one-electron-reduced G:C base pair by water. Through the calculations of thermochemical cycles, the protonation free energies were estimated to be in the range of 11.6–14.2 kcal/mol. The calculations for the models of $C^{\bullet-}(H_2O)_8$ and $G(-H1)^-(H_2O)_{16}$, which were used to simulate the detailed processes of protonation by water before and after the interbase proton transfer, respectively, revealed that the protonation proceeds through a concerted double proton transfer involving the water molecules in the first and second hydration shells. Comparing the present results with the rates of interbase proton transfer and charge transfer along DNA suggests that protonation on the $C^{\bullet-}$ moiety is not competitive with interbase proton transfer, but the possibility of protonation on the $G(-H1)^-$ moiety after interbase proton transfer cannot be excluded. Electronic-excited-state calculations were also carried out by the time-dependent DFT approach. This information is valuable for experimental identification in the future.

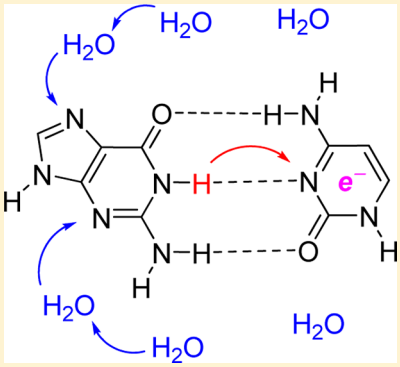

INTRODUCTION

Ionization-induced proton transfer in DNA continues to be an active research theme because of the connection with charge transport[1−4] and radiation damage of DNA.[5−9] When nucleobases are oxidized by removing an electron or reduced by adding an electron, their acid–base properties are changed, which might therefore give rise to a shift of the prototropic equilibria in base pairs. In light of their relative ionization potentials and electron affinities, adenine (A) and guanine (G) are the preferred sites on which positive holes accumulate, whereas excess electrons favor thymine (T) and cytosine (C).[10−12] Early pK_a measurements suggested that, in $G^{\bullet+}$:C and G:$C^{\bullet-}$, the proton in the middle hydrogen bond tends to transfer onto the cytosine moiety, namely, that the prototropic equilibria are shifted to the interbase proton-transferred structures of $G(-H1)^{\bullet}$:$C(H3)^+$ and $G(-H1)^-$:$C(H3)^{\bullet}$ (see Figure 1 for atom numbering).[13−15] In contrast with G:C, analogous ionization-induced interbase proton transfers in A:T were inferred to be energetically unfavorable.[13,15]

The earlier inference from pK_a measurements has been confirmed by numerous computational and experimental studies. Regarding the base pair radical anion, density functional theory (DFT) calculations on isolated G:$C^{\bullet-}$ showed that interbase proton transfer is an exothermic reaction with a small energetic barrier in the gas phase and in aqueous environments.[16−18] Szyperska et al. employed gas-phase photoelectron spectroscopy and quantum chemical calculations to study the radical anions of 9-methylguanine:1-methylcytosine, and their results established that the detected species exist in the proton-transferred structure.[19] A more elaborate model embedding G:$C^{\bullet-}$ in the B-form DNA environment was also investigated by Chen and co-workers by the DFT approach.[20,21] They reported that the excess electron is localized on a single G:C base pair and the energetics of interbase proton transfer can be significantly affected by neighboring base pairs. The reaction energies of interbase proton transfer in different sequences can differ by 10 kcal/mol in the gas phase. However, the effects of neighboring base pairs, which arise from electrostatic interactions, are largely screened upon hydration. Consequently, the sequence dependence of interbase proton transfer becomes very weak in aqueous environments.[20,21]

For base pair radical cations, an earlier DFT study on isolated $G^{\bullet+}$:C in the gas phase predicted that interbase proton transfer is endothermic,[16] conflicting with the above-mentioned pK_a measurements. The controversy was settled by later DFT and ab initio MP2 calculations, which showed that, upon incorporation of 11 water molecules around the G:C radical cation, the interbase proton-transfer reaction becomes exothermic.[22,23] A recent electron spin resonance (ESR)

Received: January 10, 2013
Revised: January 28, 2013
Published: January 30, 2013

dx.doi.org/10.1021/jp400299v | J. Phys. Chem. B 2013, 117, 2096–2105

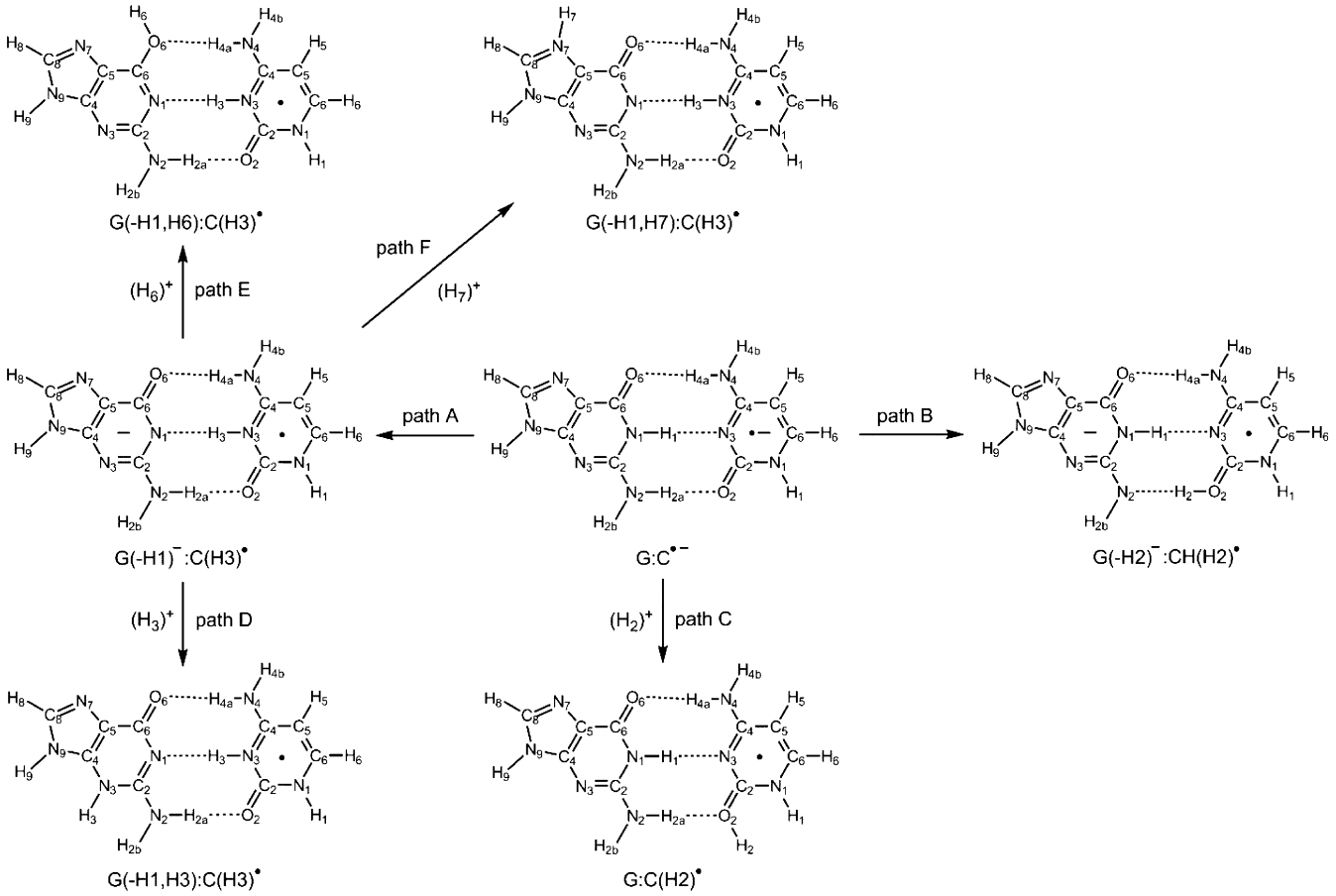

Figure 1. Possible proton-transfer pathways for the G:C$^{\bullet-}$ base pair radical anion.

study of DNA oligomers at 77 K supported the conclusion that the positive hole is localized on a single G and the resultant one-electron-oxidized G:C base pair exists entirely in the proton-transferred form.[24] However, one should keep in mind that a prototropic equilibrium between G$^{\bullet+}$:C and G(−H1)$^{\bullet}$:C-(H3)$^{+}$ would be established at room temperature, even though the proton-transferred species is still more favored.

In fact, prototropic equilibria in ionized DNA are even more complicated when considering the participation of the surrounding water molecules. This is because the water not only can alter the energetics of the interbase proton transfer but also have the potential to protonate or deprotonate the ionized nucleobases.[23,25,26] The pulse radiolysis technique combined with transient spectroscopy was used to investigate the dynamics of guanine radical cation in double-stranded oligonucleotides.[27,28] The transient species, characterized by a broad absorption at wavelengths longer than 600 nm, was assigned to the deprotonated neutral radical of G(−H1)$^{\bullet}$:C-(H3,−H4b), which was formed through interbase proton transfer from N1 of G to N3 of C, followed by release of a proton to the surrounding water from the exocyclic amino group of C. The rate constants of deprotonation by water were determined to be in the range of 10^6−10^7 s^{-1},[28] which can compete with the hole-transfer process (10^4−10^{10} s^{-1})[29−36] and the irreversible water addition reaction (10^4 s^{-1}).[37] The deprotonation of one-electron-oxidized G:C by water was also simulated using quantum chemical calculations on the model of the G:C radical cation surrounded by 11 water molecules; the activation free energy was estimated to be ca. 12 kcal/mol.[23] Moreover, other deprotonated forms of G:C radical cation were also identified at pH ∼9 by ESR and UV−vis spectral studies.[38] In that work, the deprotonated form of G(−H1)$^{\bullet}$:C was detected at 155 K and was proposed to be in a sliding base-pairing configuration predicted by theory, whereas the coexistence of G(−H1)$^{\bullet}$:C and G(−H2b)$^{\bullet}$:C was observed upon annealing to 175 K. DFT calculations supported the conclusion that these two deprotonated species are both energetically attainable.[39,40] Recently, a computational study of one-electron-oxidized deoxyguanosine (dG$^{\bullet+}$) in double-stranded DNA pointed out that the pH of the environment exerts very different influences on the interbase proton transfer within dG$^{\bullet+}$:dC and the proton transfer between dG$^{\bullet+}$ and surrounding water. At a physiological pH of 7.4, the latter was found to be dominant over the former in terms of conditional equilibrium constants, and the deprotonation was found to occur mainly at the sugar moiety.[41] Accordingly, there is sufficient evidence in the literature to conclude that water can act as a proton acceptor to deprotonate one-electron-oxidized G:C base pairs.

By contrast, the role of water in the prototropic equilibrium of the one-electron-reduced G:C base pair is less understood because of limited studies. Up to now, no study has been published to demonstrate that the protonation of G:C radical anion by the surrounding water takes place. The transient absorption spectrum of excess electrons in double-stranded oligonucleotide 5′-CGGCCCGGCGC-3′ has been measured by nanosecond pulse radiolysis.[42] The spectrum exhibits a broad characteristic absorption at 450 nm and at wavelengths longer than 600 nm. Because the spectrum does not change with time, it was regarded as corresponding to the interbase

dx.doi.org/10.1021/jp400299v | J. Phys. Chem. B 2013, 117, 2096−2105

proton-transferred structure, $G(-H1)^-$:$C(H3)^\bullet$, formed instantly after the pulse. [The rate of the interbase proton transfer, $G{:}C^{\bullet-} \rightarrow G(-H1)^-{:}C(H3)^\bullet$, has been estimated to be ca. 10^{11} s^{-1},[20] beyond the detection limit of the pulse radiolysis experiments.] On the theoretical side, although several computational studies on the microhydrated G:C radical anion have been reported,[18,20,43−45] none of these works considered proton transfer between $G{:}C^{\bullet-}$ and the surrounding water.

In this work, we used proper thermochemical cycles to estimate the free energies of the protonation of the one-electron-reduced G:C base pair by water. The detailed processes of proton transfer from the surrounding water to the one-electron-reduced G:C base pair before and after interbase proton transfer were also explored using microhydrated models of $C^{\bullet-}\cdot 8H_2O$ and $G(-H1)^-\cdot 16H_2O$, respectively. The computational results suggest that one-electron-reduced G:C can be protonated by water in some DNA sequences where electron transport is inefficient. Electronic excitations of different protonation states were calculated as well and are expected to be valuable for experimental identifications in the future.

COMPUTATIONAL METHODS

Geometry optimizations and vibrational frequency calculations were carried out at the B3LYP/6-31++G** level. The performance of the B3LYP functional in describing hydrogen-bonding structures,[46−51] electron-attachment-induced proton transfer,[52−61] and excess electron binding energies[62] has been verified and, therefore, is suitable for this study. The natures of the stationary points were confirmed by vibrational frequency analyses, and the vibrational motions of the imaginary modes for the transition states were further checked with a graphical program to ensure that they connected the proper reactants and products (Figures S6−S9, Supporting Information). The thermal corrections to Gibbs free energies were made at the standard conditions of 298.15 K and 1 atm using the unscaled frequencies. The SMD version[63] of the polarizable continuum model (PCM) was used to treat the environment of bulk hydration (dielectric constant ε = 78.3553). The SMD method has been recommended for computing solvation free energies. The charge distributions were analyzed by natural population analysis. The vertical detachment energies were evaluated as the difference in total electronic energy between the neutral and anionic molecules with both in the optimized geometry of the anion. The excited-state calculations were performed at the time-dependent (TD) B3LYP/6-311++G** level and at the CAM-B3LYP/6-311++G** level using the B3LYP/6-31++G**-optimized geometries. The effect of bulk hydration was incorporated in these excited calculations. All calculations were performed with the Gaussian 09 suite of programs.[64]

The rate constants of the proton-transfer reactions between water and nucleobases were roughly estimated by the formula

$$k_{pt} = \nu e^{-\Delta G^*/RT}$$

where ν is the bond-stretching frequency of water molecule, which was assumed to be 3500 cm^{-1}, and ΔG^* is the activation free energy.

RESULTS AND DISCUSSION

Proton-Transfer Pathway. The reversible proton-transfer pathways of the one-electron-reduced G:C base pair are depicted in Figure 1. Paths A and B correspond to the interbase proton transfers along the central N1(G)−H···N3(C) hydrogen bond and the peripheral N2(G)−H···O2(C) hydrogen bond, respectively. Previous studies have shown that the latter is energetically unfavorable and cannot compete with the former.[21] Accordingly, the subsequent protonation steps following path B were not considered in this work. Before the interbase proton transfer, the negative charges populated on the C moiety can trigger a proton transfer from the surrounding water to O2 of C (path C). Once the proton shifts from N1 of G to N3 of C (path A), the N1-deprotonated guanine becomes negatively charged and might, in turn, be further protonated by water at the N3 (path D), O6 (path E), and N7 (path F) sites.

Hydration Free Energy. Thermochemical cycle 1 (Scheme 1) was used to evaluate the protonation free energies of G:C

Scheme 1. Thermochemical Cycle 1

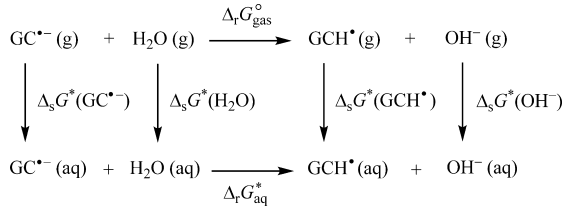

radical anion in the aqueous phase. The upper chemical equation describes the gas-phase reaction of G:C radical anion protonated by a single water molecule, resulting in the formation of neutral protonated G:C radical and hydroxide anion. The lower chemical equation, which takes into account the hydration free energy of each species, represents the corresponding reaction in aqueous solution. According to thermochemical cycle 1, the protonation free energy in aqueous solution is equal to the protonation free energy in the gas phase plus the difference in the hydration free energies between the products and reactants

$$\Delta_r G^*_{aq} = \Delta_r G^\circ_{gas} + \Delta_s G^*(GCH^\bullet) + \Delta_s G^*(OH^-) - \Delta_s G^*(GC^{\bullet-}) - \Delta_s G^*(H_2O) \quad (1)$$

The superscript symbols ° and * denote the standard states of 1 atm in the gas phase and 1 M in the solution phase, respectively. The hydration free energies of hydroxide ion and a single water molecule have been measured experimentally and amount to −104.7[65] and −6.3[66] kcal/mol, respectively. However, the experimental data for the hydration free energies of the G:C radical anion and its protonated neutral radicals are not available and needed to be estimated by computational approaches.

Accurate evaluation of solvation free energies is still a challenge in computational chemistry. Low-cost implicit solvation models have been developed and parametrized to reproduce solvation free energies.[67,68] In these models, the solvent is treated as a polarizable continuum medium, and the solvation effect is simulated by the electrostatic interaction between the polarity of the solute and the polarization charges of the medium. The drawback of continuum solvation models is that they ignore specific short-range interactions of solute with solvent, such as hydrogen-bonding and charge-transfer interactions. For the G:C base pair in duplex DNA, the O2(C), H2b(G), and N3(G) sites exposed to the minor groove and the

dx.doi.org/10.1021/jp400299v | J. Phys. Chem. B 2013, 117, 2096−2105

H4b(C), O6(G), and N7(G) sites exposed to the major groove are accessible by water. It has been shown that ca. 0.13|e| negative charge is transferred from G:C$^{\bullet-}$ to the water molecules within the first hydration shell through hydrogen-bonding interactions.[18]

To take into account the effect of the specific solute−solvent interactions, we used a supermolecule-continuum approach and thermochemical cycle 2 (Scheme 2) to estimate the hydration

Scheme 2. Thermochemical Cycle 2

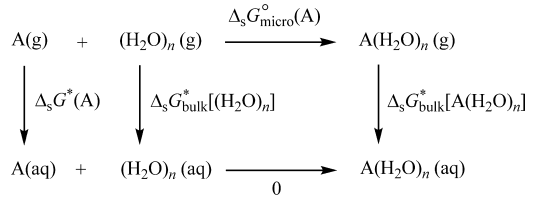

free energies of the G:C radical anion and its protonated neutral radicals. In this approach, explicit water molecules are added to fill the first hydration shell of the solute, and the remaining bulk water is treated by the SMD continuum model. According to thermochemical cycle 2, the hydration free energy is partitioned into contributions from microhydration, $\Delta_sG^\circ_{micro}(A)$, and from bulk hydration, $\Delta_sG^*_{bulk}[A(H_2O)_n]$ and $\Delta_sG^*_{bulk}[(H_2O)_n]$, as follows

$$\Delta_sG^*(A) = \Delta_sG^\circ_{micro}(A) + \Delta_sG^*_{bulk}[A(H_2O)_n] - \Delta_sG^*_{bulk}[(H_2O)_n] - \Delta G^{\circ\rightarrow *} \quad (2)$$

The last term, $\Delta G^{\circ\rightarrow *} = RT\ \ln(24.46)$, is a correction for transforming the gas-phase standard state of 1 atm to the solution-phase standard state of 1 M, which equals 1.9 kcal/mol at 298.15 K. The symbol A represents either G:C radical anions or their protonated neutral radicals.

Eight water molecules were incorporated to fill the first hydration shell of the G:C radical anions and their protonated neutral radicals. The optimized geometries are shown in Figure 2. Initial positions and orientations of the surrounding water molecules were arranged in a manner such that each proton-donor and proton-acceptor site of G:C radical anions and their protonated neutral radicals was coordinated by a water molecule and the water molecules were connected to each other through hydrogen bonds if possible. For the water cluster of $(H_2O)_8$, the global minimum is a cuboid structure of D_{2d} symmetry.[69,70] We also calculated the hydration free energy of hydroxide ion for comparison with the experimental value. Vibrational spectra recorded by argon predissociation spectroscopy revealed that the first hydration shell of the hydroxide ion contains three water molecules.[71] We therefore used the model of $OH^-(H_2O)_3$ to calculate the hydration free energy of OH^-. The global minimum of $(H_2O)_3$ is a cyclic structure.[69]

The calculated hydration free energies are summarized in Table 1. It is surprising that the hydration free energy of OH^- calculated by the supermolecule-continuum model exactly matches the experimental value of −104.7 kcal/mol. Although this result is fortuitous, it convinces us that the hydration free energies evaluated by such an approach are reliable to some extent. The hydration free energy of OH^- calculated using only the SMD model is underestimated by 10 kcal/mol because of the neglect of the influence of specific short-range interactions between OH^- and surrounding water molecules. Analysis of the charge distribution reveals that 0.25|e| negative charge shifts

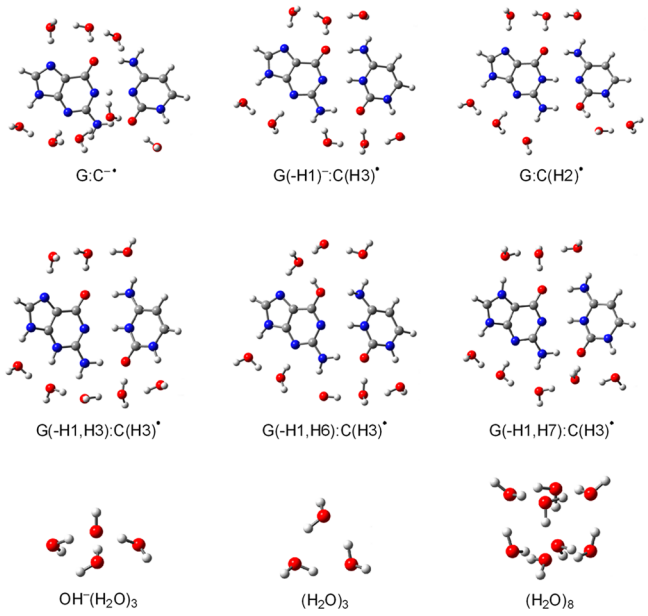

Figure 2. Microhydrated structures optimized at the B3LYP/6-31++G** level. These structures were employed to evaluate the hydration free energies of G:C$^{\bullet-}$, G(−H1)$^-$:C(H3)$^\bullet$, their protonated neutral radicals, and OH^- through thermochemical cycle 2.

from OH^- to the three coordinated water molecules. The hydration free energies of G:C$^{\bullet-}$ and G(−H1)$^-$:C(H3)$^\bullet$ are −63.7 and −64.6 kcal/mol, respectively, considerably larger than those of the protonated neutral radicals, which range from −19.3 to −32.4 kcal/mol. In contrast with the case of OH^-, the performance of the SMD-only approach in estimating the hydration free energy of G:C-related systems is much improved, possibly because the extent of charge transfer between the solutes and the surrounding water is relatively smaller in these systems (0.02−0.18|e|). However, the largest deviation from the estimation of the supermolecule-continuum approach, occurring for the system of G(−H1,H6):C(H3)$^\bullet$, still reaches 4.4 kcal/mol. Except for OH^-, the major contributions of the hydration free energies of the G:C-related systems come from bulk hydration. For G:C(H2)$^\bullet$ and G(−H1,H6):C(H3)$^\bullet$, microhydration is even a slightly endergonic process, reflecting the fact that the stabilization energy gained from the formation of the hydrogen bonds between the base pair and the water molecules cannot compensate for the energy cost of breaking the hydrogen-bonding network between the water molecules.

For comparison, we also utilized the conductor-like polarizable continuum model (CPCM)[72,73] to calculate the hydration free energies (Table S1 and Figure S1, Supporting Information). Although a linear correlation exists between the results of SMD and CPCM (Figure S1, Supporting Information), indicating that the trends in the relative magnitudes of hydration free energies predicted by the two solvation models are consistent, the absolute values derived from the CPCM calculations are systematically smaller than those derived from the SMD calculations (Table S1, Supporting Information). For the calculations using only the implicit solvation model, the deviations between the SMD and CPCM results are quite large, ranging from 8.3 to 11.9 kcal/mol with an average deviation of 9.9 kcal/mol. Including explicit water molecules in the first hydration shell does not help much, only slightly reducing the deviations to the range of

dx.doi.org/10.1021/jp400299v | J. Phys. Chem. B 2013, 117, 2096−2105

Table 1. Microhydrated, Bulk, and Total Hydration Free Energies (kcal/mol)

	$\Delta_s G^\circ_{micro}(A)$	$\Delta_s G^\circ_{bulk}[A(H_2O)_8]$	$\Delta_s G^*(A)^a$
OH^-	−48.3	−67.9	−104.7 (−94.7)
$G:C^{\bullet -}$	−11.9	−69.6	−63.7 (−63.8)
$G(-H1)^-:C(H3)^\bullet$	−13.5	−68.9	−64.6 (−65.4)
$G:C(H2)^\bullet$	1.6	−51.8	−32.4 (−30.9)
$G(-H1,H3):C(H3)^\bullet$	−2.6	−46.0	−30.8 (−34.9)
$G(-H1,H6):C(H3)^\bullet$	1.1	−38.2	−19.3 (−23.7)
$G(-H1,H7):C(H3)^\bullet$	−7.6	−41.2	−31.0 (−34.5)

[a]The values in parentheses were calculated by using only the SMD model without explicit water molecules.

3.1−9.0 kcal/mol and the average deviation to 7.1 kcal/mol. The results of the PCM calculations are almost identical to those of the CPCM calculations and, therefore, are not reported.

Protonation Free Energy. The calculated free energy changes for protonation of the one-electron-reduced G:C base pair are listed in Table 2. In the gas phase, the protonation reactions are highly endergonic, as a fairly high energy is required to break the O−H bond of a water molecule. The gas-phase protonation free energies were calculated to be in the range of 66.6−81.3 kcal/mol. Nevertheless, in the aqueous phase, the resultant OH^- ion can be solvated by water and releases 104.7 kcal/mol hydration energy. As a consequence, the endergonicities of the protonation of the one-electron-reduced G:C base pair are significantly lowered to the range of 11.6−14.2 kcal/mol. The energetically lowest protonation site in the gas phase is different from that in the aqueous phase; the former occurs at O6, and the latter occurs at N3 of the N1-deprotonated guanine moiety. This result suggests that solvation could alter the preferred site of protonation for a molecule. Whereas the protonation energies calculated by the supermolecule-continuum and the SMD-only approaches are different in absolute values, their trends are consistent. Accordingly, to determine the preferred site of protonation for a molecule in solution, solvent effects have to be considered, at least with the continuum solvation model.

Table 2. Gas-Phase and Aqueous-Phase Protonation Free Energies (kcal/mol)

	$\Delta_r G^\circ_{gas}$	$\Delta_r G^*_{aq}$	$\Delta_r G^*_{aq}$(SMD-only)
$G:C(H2)^\bullet$	81.3	14.2	15.8
$G(-H1,H3):C(H3)^\bullet$	76.2	11.6	8.3
$G(-H1,H6):C(H3)^\bullet$	66.6	13.5	9.9
$G(-H1,H7):C(H3)^\bullet$	77.2	12.4	9.7

Protonation Mechanism. We further used the cytosine radical anion solvated by eight water molecules, $C^{\bullet -}(H_2O)_8$, and the N1-deprotonated guanine anion solvated by 16 water molecules, $G(-H1)^-(H_2O)_{16}$, as the models to simulate the detailed processes of the proton transfer from the surrounding water to the one-electron-reduced G:C base pair before and after interbase proton transfer, respectively.

The optimized structures before and after protonation and the corresponding transition-state structures are shown in Figures 3 and 4. The protonations of $C^{\bullet -}$ and $G(-H1)^-$ by water were found to be achieved by a mechanism of concerted double proton transfer. During the proton transfer from the H_2O in the first hydration shell to the nucleobase, the H_2O in the second hydration shell simultaneously hands over its proton to stabilize the partially dissociated H_2O in the first hydration shell. Through this mechanism, the resultant OH^- ion is transferred to the second hydration shell and fully solvated by three water molecules, in turn lowering the reaction energy. Our computational experiences showed that, to successfully locate the protonated structures, the number of explicit water molecules and their arrangements had to meet a critical condition that the resultant OH^- ion must be fully solvated by three water molecules after the double proton transfer. In addition, the geometry optimizations had to be performed under the inclusion of bulk hydration using the SMD method; otherwise, the local minima corresponding to the protonated states also did not exist. These results reflect the important role played by the hydration of OH^- in lowering the energy of the protonated states, as revealed by the analysis of the thermochemical cycles mentioned above.

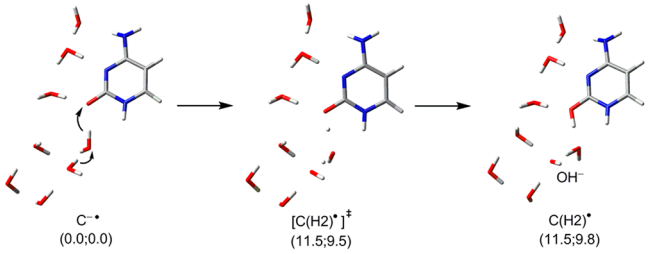

Figure 3. SMD/B3LYP/6-31++G**-optimized structures for proton transfer from water to O2 of cytosine radical anion. The values in parentheses are relative total energies and Gibbs free energies, respectively, in kcal/mol.

The forward barriers of proton transfer from water to $C^{\bullet -}$ and $G(-H1)^-$ were calculated to be in the range of 10.4−14.3 kcal/mol (Figures 3 and 4). On the other hand, the local minima of the protonated states were found to be quite shallow because the backward barriers were only within 1.2 kcal/mol and could be easily overcome at room temperature. In fact, thermal corrections to free energies at 298.15 K make the protonated states higher in energy than the corresponding transition states (Figures 3 and 4). The endergonicities of the protonation of $C^{\bullet -}$ and $G(-H1)^-$ fall in the range of 9.0−12.5 kcal/mol. These values are systematically smaller than those derived from the calculations of thermochemical cycles, possibly because the influences of the complementary bases are missing in the calculations of $C^{\bullet -}(H_2O)_8$ and $G(-H1)^-(H_2O)_{16}$. The shallowness of the local minima corresponding to the protonated states appears to imply that these states are dynamically unstable against reverse proton transfer.[74,75] However, one should keep in mind that the transport mechanism of OH^- ion in aqueous solution is very unique and efficient, with an activation energy of ca. 3 kcal/mol,[76,77] competitive with the reverse proton-transfer reaction. Thus, once the protonation of the one-electron-reduced G:C

dx.doi.org/10.1021/jp400299v | J. Phys. Chem. B 2013, 117, 2096−2105

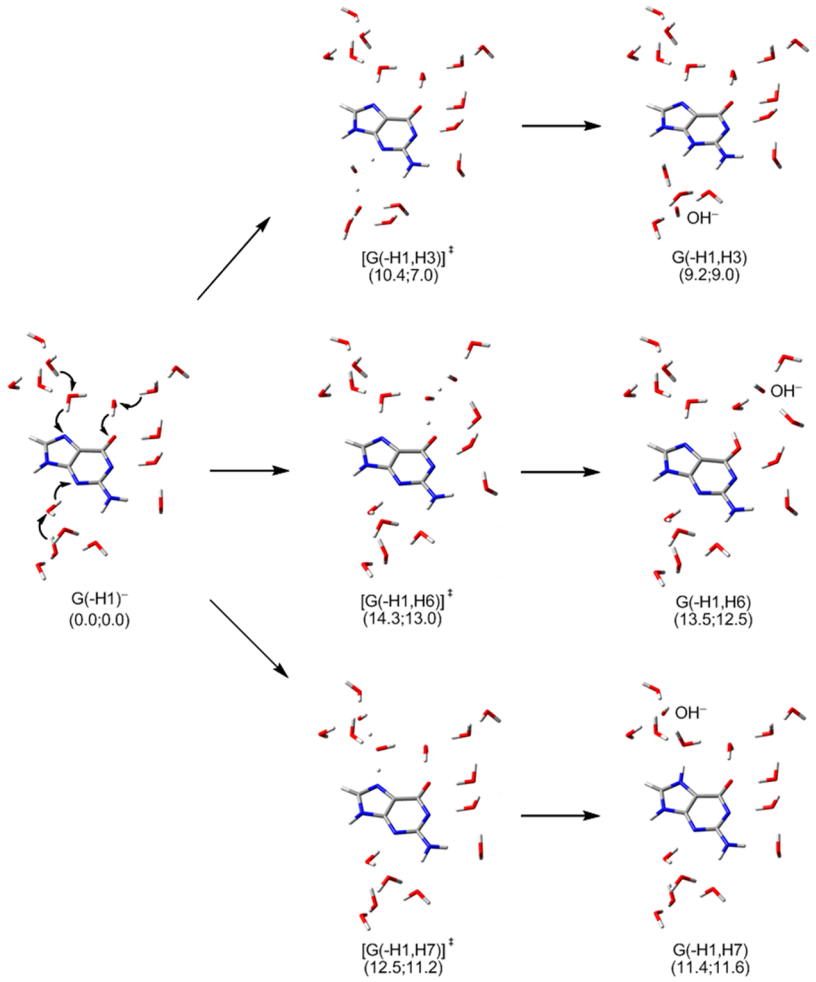

Figure 4. SMD/B3LYP/6-31++G**-optimized structures for proton transfer from water to N3 (top), O6 (middle), and N7 (bottom) of N1-deprotonated guanine anion. The values in parentheses are relative total energies and Gibbs free energies, respectively, in kcal/mol.

base pair occurs, the resulting OH^- ion in the second hydration shell has a chance to further diffuse into the bulk water and escape from recombination with the releasing H^+.

To test the sensitivity of the computational results to the number of water molecules, we also calculated the protonation reactions in the models of $C^{\bullet-}(H_2O)_9$ and $G(-H1)^-(H_2O)_{11}$ (Figures S2 and S3, Supporting Information). These results, compared with those for $C^{\bullet-}(H_2O)_8$ and $G(-H1)^-(H_2O)_{16}$ (Figures 3 and 4), demonstrate that the influence of the water molecules far from the protonation site is not significant. Accordingly, the conclusions that proton transfer from water to the one-electron-reduced G:C base pair is an endergonic process and the protonated states are quite shallow on the potential energy surfaces are not altered by changing the number of water molecules around the sites that are not directly involved in the protonation. However, as mentioned above, the water molecules around the protonation site play a critical role in determining the energetics of the protonation process through interactions with the OH^- ion.

Protonation Rate. Because proton transfer from water to one-electron-reduced G:C was found to be endergonic and the reverse barrier vanished after thermal correction, in such a case, the endergonicity of the reaction can be considered as the activation free energy. Therefore, using the endergonicities derived from the calculations of thermochemical cycles, the rate constants of the protonation steps can be roughly estimated. The rate of protonation at the O2 site of the $C^{\bullet-}$ moiety prior to interbase proton transfer is ca. 10^3 s^{-1}. This process obviously cannot rival the interbase proton transfer of $G{:}C^{\bullet-} \rightarrow G(-H1)^-{:}C(H3)^{\bullet}$, for which the rate was estimated to be 10^{11} s^{-1}.[20] On the other hand, the rates of protonation at the N3, O6, and N7 sites of the $G(-H1)^-$ moiety after interbase proton transfer were calculated to be in the range of 10^4–10^5 s^{-1}. These protonation processes must compete with electron transfer along DNA. Unfortunately, the measurement of the rate constant for electron transfer in DNA is extremely limited so far. To our knowledge, only the electron-hopping rate in a consecutive T sequence was determined to be on the order of 10^{10} s^{-1}.[78] In contrast to electron transfer, the dynamics for hole transfer along DNA has been widely investigated, and abundant data for hole-transfer rates are available. Hole transfers in DNA have been measured to occur with the rates of 10^4–10^{10} s^{-1}, depending on the sequences.[27−34] If we venture to assume that electron transfers along DNA take place in a similar time range as hole transfers, then $G(-H1)^-{:}C(H3)^{\bullet}$ is likely to be further protonated by the surrounding water molecules in some DNA sequences where electron transfers are inefficient.

Quantum tunneling effects have been demonstrated to be important in the proton-transfer reactions within a double-well potential.[79] However, in the present cases, the local minima of the products (i.e., the protonated states) are extremely shallow

dx.doi.org/10.1021/jp400299v | J. Phys. Chem. B 2013, 117, 2096−2105

and higher in energy than the reactants. In other words, proton transfer from water to one-electron-reduced G:C should be classified as the reaction of a single-well potential in which proton tunneling is not expected to occur.

Vertical Detachment Energy (VDE). The protonation state has a substantial influence on the electron binding energy of a base pair radical anion, which is an important physical quantity associated with the efficiency of electron transfer. The vertical detachment energies (VDEs) for different protonation states of one-electron-reduced G:C in the aqueous phase are summarized in Table 3. The computational results indicate that

Table 3. Aqueous-Phase Vertical Detachment Energies (eV)

	present study[a]	ref 43
$G:C^{\bullet-}$	2.502	1.84,[b,c] 1.87,[b,e] 2.28,[c,d] 2.32[d,e]
$G(-H1)^{-}:C(H3)^{\bullet}$	2.848	
$G:C(H2)^{\bullet}$	2.835	
$G(-H1,H3):C(H3)^{\bullet}$	2.971	
$G(-H1,H6):C(H3)^{\bullet}$	2.989	
$G(-H1,H7):C(H3)^{\bullet}$	2.963	

[a]Calculations included eight explicit water molecules in the first hydration shell and the bulk hydration described by the SMD model. [b]Calculations included six explicit water molecules. [c]B3LYP/6-31+G**. [d]Calculations included 11 explicit water molecules. [e]BHandHLYP/6-31+G**//B3LYP/6-31+G**.

the VDE is significantly increased from 2.502 eV for $G:C^{\bullet-}$ to 2.848 eV for $G(-H1)^{-}:C(H3)^{\bullet}$. This could be the reason why electron transfer along a poly-T tract is more efficient than that along a poly-C tract, because interbase proton transfer is unlikely to occur in the A:T base pair. Protonations on the $G(-H1)^{-}$ moiety were found to be able to further stabilize the excess electron on the $C(H3)^{\bullet}$ moiety. The VDEs increased by 0.123, 0.141, and 0.115 eV upon protonations at the N3, O6, and N7 sites, respectively, of $G(-H1)^{-}$. These results indicate that electron transfer can be regulated by protonation on the complementary base of the charge carrier. We note that Kumar and co-workers reported the VDEs of $G:C^{\bullet-}$ in the presence of 6 and 11 water molecules to be ca. 1.8 and 2.3 eV, respectively.[43] These values are somewhat smaller than the results of our calculations including eight water molecules and PCM-treated bulk hydration.

Excited-State Properties. The excited-state properties of one-electron-reduced G:C base pair and its protonated neutral radicals were calculated using the TD-DFT approach combined with the B3LYP functional (Table S2 and Figure S4, Supporting Information) and the long-range corrected CAM-B3LYP functional (Table 4 and Figure 5; Table S3 and Figure S5, Supporting Information).

The TD-DFT computational results for B3LYP and CAM-B3LYP are markedly different. On the whole, the B3LYP functional predicts more charge-transfer (CT) and Rydberg excited states and dramatically underestimates the excitation energies of the CT excited states in comparison with the CAM-B3LYP functional. Because it is well-known that standard exchange-correlation functionals, such as B3LYP, provide incorrect descriptions for CT excited states,[80−82] the following discussion is based on the CAM-B3LYP results.

The excited states of the one-electron-reduced G:C base pair and its protonated neutral radicals involve the mixing of many transition configurations with moderate or low contributions and, therefore, makes the assignment of the excited-state

Table 4. Excitation Wavelengths λ, Oscillator Strengths *f*, and Excitation Natures Calculated by the SMD/TD-DFT/CAM-B3LYP/6-311++G Method[a]**

protonation state	λ (nm/eV)	*f*	assignment[b]
$G:C^{\bullet-}$	646/1.919	0.0084	C-π* → C-π*
	517/2.398	0.0039	C-π* → C-Rydberg
	412/3.009	0.0085	C-π* → G-π*
$G(-H1)^{-}:C(H3)^{\bullet}$	583/2.127	0.0088	C-π* → C-π*
	447/2.774	0.0042	C-π* → C-Rydberg
	354/3.502	0.0034	C-π* → C-Rydberg
$G:C(H2)^{\bullet}$	671/1.848	0.0064	C-π* → C-π*
	460/2.695	0.0030	C-π* → C-Rydberg
$G(-H1,H3):C(H3)^{\bullet}$	579/2.141	0.0080	C-π* → C-π*
	432/2.870	0.0042	C-π* → C-Rydberg
	376/3.297	0.0042	C-π* → G-π*
$G(-H1,H6):C(H3)^{\bullet}$	567/2.187	0.0082	C-π* → C-π*
	431/2.877	0.0035	C-π* → C-Rydberg
$G(-H1,H7):C(H3)^{\bullet}$	575/2.156	0.0081	C-π* → C-π*
	435/2.850	0.0036	C-π* → C-Rydberg
	372/3.333	0.0084	C-π* → G-π*

[a]Only excitations with λ > 350 nm and *f* > 0.0030 are reported. [b]Assignment based on the natural transition orbital analysis. See Figure 5.

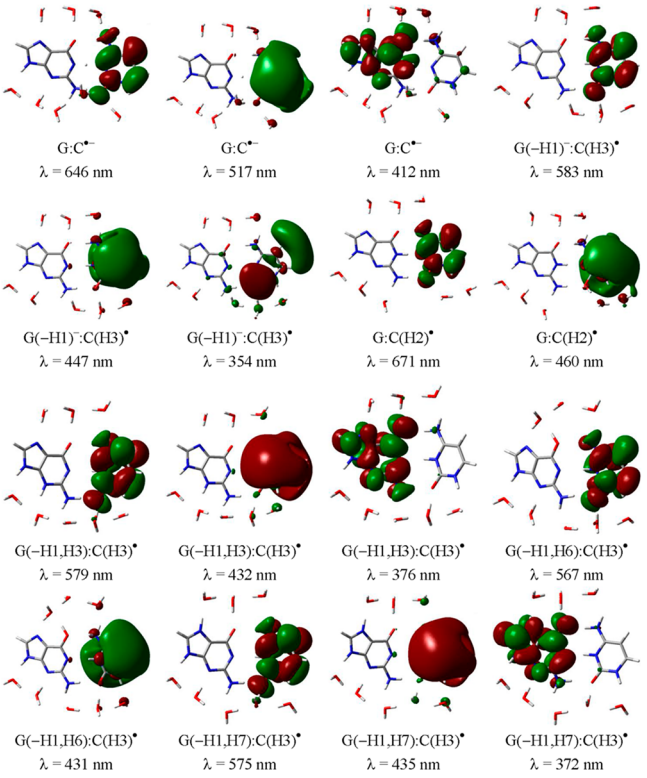

Figure 5. Natural transition orbital analysis for the TD-DFT calculations at the SMD/CAM-B3LYP/6-311++G** level.

characteristics difficult (Table S3 and Figure S5, Supporting Information). We thus performed natural transition orbital (NTO) analysis,[83] and the results show that all of these excited states can be well represented by a single transition between two NTOs (contribution > 98%). Because all of the excitations originate from the excess electron on the π* orbital of C, these initial NTOs are not depicted, and only the destination NTOs are shown in Figure 5.

dx.doi.org/10.1021/jp400299v | J. Phys. Chem. B 2013, 117, 2096−2105

The one-electron-reduced G:C base pair and its protonated neutral radicals exhibit three types of absorption within the range of visible light: local excitation from π^* to π^* of C, local excitation from π^* to the Rydberg state of C, and CT excitation from π^* of C to π^* of G (Table 4). The C-π^* → C-π^* excited states are lowest in energy, with absorption wavelengths (λ) ranging from 567 to 646 nm. The next excited states are the Rydberg states of the C moiety, with λ = 354−517 nm. The highest excited states are the CT excited states of C-π^* → G-π^*, for which the corresponding wavelengths are within the range of 372−412 nm. It is noteworthy that the CT excitation of C-π^* → G-π^*, which is originally located at 412 nm in G:C$^{\bullet-}$, is blue-shifted over λ < 350 nm in G(−H1)$^-$:C(H3)$^\bullet$. Upon protonation on the N3 and N7 sites of the G(−H1)$^-$ moiety, the CT excitations are recovered at 376 and 372 nm, respectively. The sensitivity of the C-π^* → G-π^* excitation to the protonation state makes it a potential spectral fingerprint for experimental identification. We notice that the Rydberg excitations of G(−H1)$^-$:C(H3)$^\bullet$ are in close proximity to the CT excitations of G:C$^{\bullet-}$, G(−H1,H3):C(H3)$^\bullet$, and G(−H1,H7):C(H3)$^\bullet$, which might render these protonation states indistinguishable in UV−vis spectra. Nevertheless, these Rydberg excited states are very diffuse (Figure 5) and, therefore, unlikely to appear in the DNA environment due to the repulsive interactions with the π electrons of neighboring bases.

The present results cannot be compared with the transient absorption spectra of the excess electron in double-stranded oligonucleotides,[42] as the intrastrand base-to-base and the base-to-sugar−phosphate backbone CT excitations are not considered in the present models. TD-DFT calculations on a more elaborate DNA model that includes other components are needed to provide more conclusive excited-state properties of the excess electron in DNA. We are now undertaking such a study.

CONCLUSIONS

The energetics and mechanism for the protonation of the one-electron-reduced G:C base pair by the surrounding water have been investigated using DFT calculations. The reactions of protonation by water were found to be endergonic by 11.6−14.2 kcal/mol, depending on the protonation site. The present results, combined with the previous findings, indicate that protonation of the C$^{\bullet-}$ moiety by water cannot compete with the interbase proton transfer of G:C$^{\bullet-}$ → G(−H1)$^-$:C(H3)$^\bullet$. However, the possibility for further protonation on the G(−H1)$^-$ moiety of G(−H1)$^-$:C(H3)$^\bullet$ in some DNA sequences where electron transfer is slow cannot be ruled out. The favorable sites for protonation are at N3 and N7 of the G(−H1)$^-$ moiety. The protonations take place through a concerted double proton transfer involving the water molecules in the first and second hydration layers. Through this mechanism, the resultant OH$^-$ ion can be fully solvated by three water molecules, which, in turn, lowers the reaction energy. TD-DFT calculations predict that the G:C base pair radical anion and its protonated neutral radicals exhibit three types of electronic excited states with increasing energy in the order C-π^* → C-π^* < C-π^* → C-Rydberg < C-π^* → G-π^*. The CT excitation of C-π^* → G-π^* is sensitive to the protonation state and might be a useful spectral fingerprint for experimental identification.

ASSOCIATED CONTENT

Supporting Information

CPCM hydration free energies, TD-DFT results, C$^{\bullet-}$(H$_2$O)$_9$ and G(−H1)$^-$(H$_2$O)$_{11}$ calculations, imaginary modes of transition states, and Cartesian coordinates of optimized structures. This material is available free of charge via the Internet at http://pubs.acs.org.

AUTHOR INFORMATION

Corresponding Author

*E-mail: hychen@kmu.edu.tw. Fax: +886 7 3125339. Tel: +886 7 3121101 ext. 2807.

Notes

The authors declare no competing financial interest.

ACKNOWLEDGMENTS

We thank the National Science Council of Taiwan for financial support and the National Center for High-Performance Computing for computer time and facilities.

REFERENCES

(1) Genereux, J. C.; Barton, J. K. Mechanisms for DNA Charge Transport. *Chem. Rev.* **2010**, *110*, 1642−1662.
(2) Giese, B.; Wessely, S. The Significance of Proton Migration during Hole Hopping through DNA. *Chem. Commun.* **2001**, *37*, 2108−2109.
(3) Cai, Z.; Li, X.; Sevilla, M. D. Excess Electron Transfer in DNA: Effect of Base Sequence and Proton Transfer. *J. Phys. Chem. B* **2002**, *106*, 2755−2762.
(4) Kawai, K.; Osakada, Y.; Majima, T. Importance of Protonation State of Guanine Radical Cation During Hole Transfer in DNA. *ChemPhysChem* **2009**, *10*, 1766−1769.
(5) Kumar, A.; Sevilla, M. D. Proton-Coupled Electron Transfer in DNA on Formation of Radiation-Produced Ion Radicals. *Chem. Rev.* **2010**, *110*, 7002−7023.
(6) Lyngdoh, R. H. D.; Schaefer, H. F., III. Elementary Lesions in DNA Subunits: Electron, Hydrogen Atom, Proton, and Hydride Transfers. *Acc. Chem. Res.* **2009**, *42*, 563−572.
(7) Gu, J.; Leszczynski, J.; Schaefer, H. F., III. Interactions of Electrons with Bare and Hydrated Biomolecules: From Nucleic Acid Bases to DNA Segments. *Chem. Rev.* **2012**, *112*, 5603−5640.
(8) Shukla, M. K., Leszczynski, J., Eds. *Radiation Induced Molecular Phenomena in Nucleic Acids: A Comprehensive Theoretical and Experimental Analysis*; Springer-Verlag: Amsterdam, 2008; pp 577−667.
(9) Kumar, A.; Sevilla, M. D. Sugar Radical Formation by a Proton Coupled Hole Transfer in 2′-Deoxyguanosine Radical Cation (2′dG$^{\bullet+}$): A Theoretical Treatment. *J. Phys. Chem. B* **2009**, *113*, 13374−13380.
(10) Seidel, C. A. M.; Schulz, A.; Sauer, M. H. M. Nucleobase-Specific Quenching of Fluorescent Dyes. 1. Nucleobase One-Electron Redox Potentials and Their Correlation with Static and Dynamic Quenching Efficiencies. *J. Phys. Chem.* **1996**, *100*, 5541−5553.
(11) Li, X.; Cai, Z.; Sevilla, M. D. Energetics of the Radicals Ions of the AT and AU Base Pairs: A Density Functional Theory (DFT) Study. *J. Phys. Chem. A* **2002**, *106*, 9345−9351.
(12) Giese, B. Long-Distance Electron Transfer through DNA. *Annu. Rev. Biochem.* **2002**, *71*, 51−70.
(13) Steenken, S.; Telo, J. P.; Novais, H. M.; Candeias, L. P. J. One-Electron-Reduction Potentials of Pyrimidines Bases, Nucleosides, and Nucleotides in Aqueous Solution. Consequences for DNA Redox Chemistry. *J. Am. Chem. Soc.* **1992**, *114*, 4701−4709.
(14) Candeias, L. P.; Steenken, S. Structure and Acid-Base Properties of One-Electron-Oxidized Deoxyguanosine, Guanosine, and 1-Methylguanosine. *J. Am. Chem. Soc.* **1989**, *111*, 1094−1099.

(15) Steenken, S. Purine Bases, Nucleosides, and Nucleotides: Aqueous Solution Redox Chemistry and Transformation Reactions of Their Radical Cations and e^- and OH Adducts. *Chem. Rev.* **1989**, *89*, 503−520.
(16) Li, X.; Cai, Z.; Sevilla, M. D. Investigation of Proton Transfer within DNA Base Pair Anion and Cation Radicals by Density Functional Theory (DFT). *J. Phys. Chem. B* **2001**, *105*, 10115−10123.
(17) Gu, J.; Xie, Y.; Schaefer, H. F., III. Electron Attachment Induced Proton Transfer in a DNA Nucleoside Pair: 2′-Deoxyguanosine-2′-Deoxycytidine. *J. Chem. Phys.* **2007**, *127*, 155107.
(18) Chen, H. Y.; Hsu, S. C. N.; Kao, C. L. Microhydration of 9-Methylguanine:1-Methylcytosine Base Pair and Its Radicals Anion: A Density Functional Theory Study. *Phys. Chem. Chem. Phys.* **2010**, *12*, 1253−1263.
(19) Szyperska, A.; Rak, J.; Leszczynski, J.; Li, X.; Ko, Y. J.; Wang, H.; Bowen, K. H. Valence Anions of 9-Methylguanine−1-Methylcytosine Complexes. Computational and Photoelectron Spectroscopy Studies. *J. Am. Chem. Soc.* **2009**, *131*, 2663−2669.
(20) Chen, H. Y.; Kao, C. L.; Hsu, S. C. N. Proton Transfer in Guanine−Cytosine Radical Anion Embedded in B-Form DNA. *J. Am. Chem. Soc.* **2009**, *131*, 15930−15938.
(21) Chen, H. Y.; Yeh, S. W.; Hsu, S. C. N.; Kao, C. L.; Dong, T. Y. Effect of Nucleobase Sequence on the Proton-Transfer Reaction and Stability of the Guanine−Cytosine Base Pair Radical Anion. *Phys. Chem. Chem. Phys.* **2011**, *13*, 2674−2681.
(22) Kumar, A.; Sevilla, M. D. Influence of Hydration on Proton Transfer in the Guanine−Cytosine Radical Cation ($G^{\bullet+}$−C) Base Pair: A Density Functional Theory Study. *J. Phys. Chem. B* **2009**, *113*, 11359−11361.
(23) Cerón-Carrasco, J. P.; Requena, A.; Perpète, E. A.; Michaux, C.; Jacquemin, D. Theoretical Study of the Tautomerism in the One-Electron Oxidized Guanine−Cytosine Base Pair. *J. Phys. Chem. B* **2010**, *114*, 13439−13445.
(24) Adhikary, A.; Khanduri, D.; Sevilla, M. D. Direct Observation of the Hole Protonation State and Hole Localization Site in DNA-Oligomers. *J. Am. Chem. Soc.* **2009**, *131*, 8614−8619.
(25) Cerón-Carrasco, J. P.; Zúñiga, J.; Requena, A.; Perpète, E. A.; Michaux, C.; Jacquemin, D. Combined Effect of Stacking and Solvation on the Spontaneous Mutation in DNA. *Phys. Chem. Chem. Phys.* **2011**, *13*, 14584−14589.
(26) Cerón-Carrasco, J. P.; Jacquemin, D. Interplay Between Hydroxyl Radical Attack and H-Bond Stability in Guanine−Cytosine. *RSC Adv.* **2012**, *2*, 11867−11875.
(27) Kobayashi, K.; Tagawa, S. Direct Observation of Guanine Radical Cation Deprotonation in Duplex DNA Using Pulse Radiolysis. *J. Am. Chem. Soc.* **2003**, *125*, 10213−10218.
(28) Kobayashi, K.; Yamagami, R.; Tagawa, S. Effect of Base Sequence and Deprotonation of Guanine Cation Radical in DNA. *J. Phys. Chem. B* **2008**, *112*, 10752−10757.
(29) Lewis, F. D.; Letsinger, R. L.; Wasielewski, M. R. Dynamics of Photoinduced Charge Transfer and Hole Transport in Synthetic DNA Hairpins. *Acc. Chem. Res.* **2001**, *34*, 159−170.
(30) Lewis, F. D.; Wu, T.; Zhang, Y.; Letsinger, R. L.; Greenfield, S. R.; Wasielewski, M. R. Direct Measurement of Hole Transport Dynamics in DNA. *Nature* **2000**, *406*, 51−53.
(31) Lewis, F. D.; Liu, J.; Zuo, X.; Hayes, R. T.; Wasielewski, M. R. Dynamics and Energetics of Single-Step Hole Transport in DNA Hairpins. *J. Am. Chem. Soc.* **2003**, *125*, 4850−4861.
(32) Takada, T.; Kawai, K.; Cai, X.; Sugimoto, A.; Fujitsuka, M.; Majima, T. Charge Separation in DNA via Consecutive Adenine Hopping. *J. Am. Chem. Soc.* **2004**, *126*, 1125−1129.
(33) Takada, T.; Kawai, K.; Fujitsuka, M.; Majima, T. Contributions of the Distance-Dependent Reorganization Energy and Proton Transfer to the Hole-Transport Process in DNA. *Chem.—Eur. J.* **2005**, *11*, 3835−3842.
(34) Osakada, Y.; Kawai, K.; Fujitsuka, M.; Majima, T. Charge Transfer through DNA Nanoscaled Assembly Programmable with DNA Building Blocks. *Proc. Natl. Acad. Sci. U.S.A.* **2006**, *103*, 18072−18076.
(35) Osakada, Y.; Kawai, K.; Fujitsuka, M.; Majima, T. Kinetics of Charge Transfer in DNA Containing a Mismatch. *Nucl. Acids Res.* **2008**, *36*, 5562−5570.
(36) Conron, S. M. M.; Thazhathveetil, A. K.; Wasielewski, M. R.; Burin, A. L.; Lewis, F. D. Direct Measurement of the Dynamics of Hole Hopping in Extended DNA G-Tracts. An Unbiased Random Walk. *J. Am. Chem. Soc.* **2010**, *132*, 14388−14390.
(37) Giese, B.; Spichty, M. Long Distance Charge Transport through DNA: Quantification and Extension of the Hopping Model. *ChemPhysChem* **2000**, *1*, 195−198.
(38) Adhikary, A.; Kumar, A.; Munafo, S. A.; Khanduri, D.; Sevilla, M. D. Prototropic Equilibria in DNA Containing One-Electron Oxidized GC: Intra-Duplex vs. Duplex to Solvent Deprotonation. *Phys. Chem. Chem. Phys.* **2010**, *12*, 5353−5368.
(39) Bera, P. P.; Schaefer, H. F., III. $(G-H)^{\bullet}$−C and G−$(C-H)^{\bullet}$ Radicals Derived From the Guanine·Cytosine Base Pair Cause DNA Subunit Lesions. *Proc. Natl. Acad. Sci. U.S.A.* **2005**, *102*, 6698−6703.
(40) Steenken, S.; Reynisson, J. DFT Calculations on the Deprotonation Site of the One-Electron Oxidised Guanine−Cytosine Base Pair. *Phys. Chem. Chem. Phys.* **2010**, *12*, 9088−9093.
(41) Galano, A.; Alvarez-Idaboy, J. R. On the Evolution of One-Electron-Oxidized Deoxyguanosine in Damaged DNA under Physiological Conditions: A DFT and ONIOM Study on Proton Transfer and Equilibrium. *Phys. Chem. Chem. Phys.* **2012**, *14*, 12476−12484.
(42) Yamagami, R.; Kobayashi, K.; Tagawa, S. Formation of Spectral Intermediate G−C and A−T Anion Complex in Duplex DNA Studied by Pulse Radiolysis. *J. Am. Chem. Soc.* **2008**, *130*, 14772−14777.
(43) Kumar, A.; Sevilla, M. D.; Suhai, S. Microhydration of the Guanine−Cytosine (GC) Base Pair in the Neutral and Anionic Radical States: A Density Functional Study. *J. Phys. Chem. B* **2008**, *112*, 5189−5198.
(44) Gu, J.; Wong, N. B.; Xie, Y.; Schaefer, H. F., III. Electron Attachment to a Hydrated DNA Duplex: The Dinucleoside Phosphate Deoxyguanylyl-3′,5′-Deoxycytidine. *Chem.—Eur. J.* **2010**, *16*, 13155−13162.
(45) Gupta, A.; Jaeger, H. M.; Compaan, K. R.; Schaefer, H. F., III. Electron Attachment to the Guanine−Cytosine Nucleic Acid Base Pair and the Effects of Monohydration and Proton Transfer. *J. Phys. Chem. B* **2012**, *116*, 5579−5587.
(46) Alfredsson, M.; OjanWe, L.; Hermansson, K. G. A Comparison of Hartree−Fock, MP2, and DFT Results for the HCN Dimer and Crystal. *Int. J. Quantum Chem.* **1996**, *60*, 767−778.
(47) Dabkowska, I.; Rak, J.; Gutowski, M. Computational Study of Hydrogen-Bonded Complexes Between the Most Stable Tautomers of Glycine and Uracil. *J. Phys. Chem. A* **2002**, *106*, 7423−7433.
(48) Rak, J.; Skurski, P.; Simons, J.; Gutowski, M. Low-Energy Tautomers and Conformers of Neutral and Protonated Arginine. *J. Am. Chem. Soc.* **2001**, *123*, 11695−11707.
(49) Dkhissi, A.; Adamowicz, L.; Maes, G. Density Functional Theory Study of the Hydrogen-Bonded Pyridine−HO Complex: A Comparison with RHF and MP2 Methods and with Experimental Data. *J. Phys. Chem. A* **2000**, *104*, 2112−2119.
(50) Makiabadi, B.; Roohi, H. Interaction Between O_3 and H_2O_2: A Theoretical Study. *Chem. Phys. Lett.* **2008**, *460*, 72−78.
(51) Simões, P. N.; Reva, I.; Pedroso, L. M.; Fausto, R.; Portugal, A. A. Low-Temperature FTIR Spectroscopic and Theoretical Study on an Energetic Nitroimine: Dinitroammeline (DNAM). *J. Phys. Chem. A* **2008**, *112*, 3432−3443.
(52) Harańczyk, M.; Bachorz, R.; Rak, J.; Gutowski, M.; Radisic, D.; Stokes, S. T.; Nilles, J. M.; Bowen, K. H. Excess Electron Attachment Induces Barrier-Free Proton Transfer in Binary Complexes of Uracil with H_2Se and H_2S but Not with H_2O. *J. Phys. Chem. B* **2003**, *107*, 7889−7895.
(53) Dąbkowska, I.; Rak, J.; Gutowski, M.; Nilles, J. M.; Stokes, S. T.; Radisic, D.; Bowen, K. H. Barrier-Free Proton Transfer in Anionic Complex of Thymine with Glycine. *Phys. Chem. Chem. Phys.* **2004**, *6*, 4351−4357.
(54) Harańczyk, M.; Dąbkowska, I.; Rak, J.; Gutowski, M.; Nilles, J. M.; Stokes, S. T.; Radisic, D.; Bowen, K. H. Excess Electron

Attachment Induces Barrier-Free Proton Transfer in Anionic Complexes of Thymine and Uracil with Formic Acid. *J. Phys. Chem. B* **2004**, *108*, 6919−6921.
(55) Dąbkowska, I.; Rak, J.; Gutowski, M.; Nilles, J. M.; Stokes, S. T.; Bowen, K. H. Barrier-Free Intermolecular Proton Transfer Induced by Excess Electron Attachment to the Complex of Alanine with Uracil. *J. Chem. Phys.* **2004**, *120*, 6064−6071.
(56) Harańczyk, M.; Rak, J.; Gutowski, M.; Radisic, D.; Stokes, S. T.; Bowen, K. H. Intermolecular Proton Transfer in Anionic Complexes of Uracil with Alcohols. *J. Phys. Chem. B* **2005**, *109*, 13383−13391.
(57) Mazurkiewicz, K.; Harańczyk, M.; Storoniak, P.; Gutowski, M.; Rak, J.; Radisic, D.; Eustis, S. N.; Wang, D.; Bowen, K. H. Intermolecular Proton Transfer Induced by Excess Electron Attachment to Adenine(Formic Acid)$_n$ (n = 2, 3) Hydrogen-Bonded Complexes. *Chem. Phys.* **2007**, *342*, 215−222.
(58) Mazurkiewicz, K.; Harańczyk, M.; Gutowski, M.; Rak, J.; Radisic, D.; Eustis, S. N.; Wang, D.; Bowen, K. H. Valence Anions in Complexes of Adenine and 9-Methyladenine with Formic Acid: Stabilization by Intermolecular Proton Transfer. *J. Am. Chem. Soc.* **2007**, *129*, 1216−1224.
(59) Radisic, D.; Bowen, K. H.; Dąbkowska, I.; Storoniak, P.; Rak, J.; Gutowski, M. AT Base Pair Anions versus (9-Methyl-A)(1-Methyl-T) Base Pair Anions. *J. Am. Chem. Soc.* **2005**, *127*, 6443−6450.
(60) Chen, H. Y.; Chao, I. Ionization-Induced Proton Transfer in Model DNA Base Pairs: A Theoretical Study of the Radical Ions of the 7-Azaindole Dimer. *ChemPhysChem* **2004**, *5*, 1855−1863.
(61) Chen, H. Y.; Young, P. Y.; Hsu, S. C. N. Theoretical Evidence of Barrier-Free Proton Transfer in 7-Azaindole−Water Cluster Anions. *J. Chem. Phys.* **2009**, *130*, 165101.
(62) Rienstra-Kiracofe, J. C.; Tschumper, G. S.; Schaefer, H. F., III. Atomic and Molecular Electron Affinities: Photoelectron Experiments and Theoretical Computations. *Chem. Rev.* **2002**, *102*, 231−282.
(63) Marenich, A. V.; Cramer, C. J.; Truhlar, D. G. Universal Solvation Model Based on Solute Electron Density and on a Continuum Model of the Solvent Defined by the Bulk Dielectric Constant and Atomic Surface Tensions. *J. Phys. Chem. B* **2009**, *113*, 6378−6396.
(64) Frisch, M. J.; Trucks, G. W.; Schlegel, H. B.; Scuseria, G. E.; Robb, M. A.; Cheeseman, J. R.; Scalmani, G.; Barone, V.; Mennucci, B.; Petersson, G. A.; Nakatsuji, H.; Caricato, M.; Li, X.; Hratchian, H. P.; Izmaylov, A. F.; Bloino, J.; Zheng, G.; Sonnenberg, J. L.; Hada, M.; Ehara, M.; Toyota, K.; Fukuda, R.; Hasegawa, J.; Ishida, M.; Nakajima, T.; Honda, Y.; Kitao, O.; Nakai, H.; Vreven, T.; Montgomery, J. A., Jr.; Peralta, J. E.; Ogliaro, F.; Bearpark, M.; Heyd, J. J.; Brothers, E.; Kudin, K. N.; Staroverov, V. N.; Keith, T.; Kobayashi, R.; Normand, J.; Raghavachari, K.; Rendell, A.; Burant, J. C.; Iyengar, S. S.; Tomasi, J.; Cossi, M.; Rega, N.; Millam, J. M.; Klene, M.; Knox, J. E.; Cross, J. B.; Bakken, V.; Adamo, C.; Jaramillo, J.; Gomperts, R.; Stratmann, R. E.; Yazyev, O.; Austin, A. J.; Cammi, R.; Pomelli, C.; Ochterski, J. W.; Martin, R. L.; Morokuma, K.; Zakrzewski, V. G.; Voth, G. A.; Salvador, P.; Dannenberg, J. J.; Dapprich, S.; Daniels, A. D.; Farkas, Ö.; Foresman, J. B.; Ortiz, J. V.; Cioslowski, J.; Fox, D. J. *Gaussian 09*, revision A.02; Gaussian, Inc.: Wallingford, CT, 2009.
(65) Kelly, C. P.; Cramer, C. J.; Truhlar, D. G. Aqueous Solvation Free Energies of Ion and Ion-Water Clusters Based on an Accurate Value for the Absolute Aqueous Solvation Free Energy of the Proton. *J. Phys. Chem. B* **2006**, *110*, 16066−16081.
(66) Camaioni, D. M.; Schwerdtfeger, C. A. Comment on "Accurate Experimental Values for the Free Energies of Hydration of H^+, OH^-, and H_3O^+". *J. Phys. Chem. A* **2005**, *109*, 10795−10797.
(67) Cramer, C. J.; Truhlar, D. G. Implicit Solvation Models: Equilibria, Structure, Spectra, and Dynamics. *Chem. Rev.* **1999**, *99*, 2161−2200.
(68) Tomasi, J.; Mennucci, B.; Cammi, R. Quantum Mechanical Continuum Solvation Models. *Chem. Rev.* **2005**, *105*, 2999−3093.
(69) James, T.; Wales, D. J.; Hernández-Rojas, J. Global Minima for Water Clusters $(H_2O)_n$, $n \leq 21$, Described by a Five-Site Empirical Potential. *Chem. Phys. Lett.* **2005**, *415*, 302−307.
(70) Day, M. B.; Kirschner, K. N.; Shields, G. C. Pople's Gaussian-3 Model Chemistry Applied to an Investigation of $(H_2O)_8$ Water Clusters. *Int. J. Quantum Chem.* **2005**, *102*, 565−572.
(71) Robertson, W. H.; Diken, E. G.; Price, E. A.; Shin, J. W.; Johnson, M. A. Spectroscopic Determination of the OH^- Solvation Shell in the $OH^-\cdot(H_2O)_n$ Clusters. *Science* **2003**, *299*, 1367−1372.
(72) Barone, V.; Cossi, M. Quantum Calculation of Molecular Energies and Energy Gradients in Solution by a Conductor Solvent Model. *J. Phys. Chem. A* **1998**, *102*, 1995−2001.
(73) Cossi, M.; Rega, N.; Scalmani, G.; Barone, V. Energies, Structures, and Electronic Properties of Molecules in Solution with the C-PCM Solvation Model. *J. Comput. Chem.* **2003**, *24*, 669−681.
(74) Gorb, L.; Podolyan, Y.; Dziekonski, P.; Sokalski, W. A.; Leszczynski, J. Double-Proton Transfer in Adenine−Thymine and Guanine−Cytosine Base Pairs. A Post-Hartree−Fock Ab Initio Study. *J. Am. Chem. Soc.* **2004**, *126*, 10119−10129.
(75) Cerón-Carrasco, J. P.; Requena, A.; Michaux, C.; Perpète, E. A.; Jacquemin, D. Effects of Hydration on the Proton Transfer Mechanism in the Adenine−Thymine Base Pair. *J. Phys. Chem. A* **2009**, *113*, 7892−7898.
(76) Agmon, N. Mechanism of Hydroxide Mobility. *Chem. Phys. Lett.* **2000**, *319*, 247−252.
(77) Tuckerman, M. E.; Marx, D.; Parrinello, M. The Nature and Transport Mechanism of Hydrated Hydroxide Ions in Aqueous Solution. *Nature* **2002**, *417*, 925−929.
(78) Park, M. J.; Fujitsuka, M.; Kawai, K.; Majima, T. Direct Measurement of the Dynamics of Excess Electron Transfer through Consecutive Thymine Sequence in DNA. *J. Am. Chem. Soc.* **2011**, *133*, 15320−15323.
(79) DiLabio, G. A.; Johnson, E. R. Lone Pair−π and π−π Interactions Play an Important Role in Proton-Coupled Electron Transfer Reactions. *J. Am. Chem. Soc.* **2007**, *129*, 6199−6203.
(80) Dreuw, A.; Head-Gordon, M. Failure of Time-Dependent Density Functional Theory for Long-Range Charge-Transfer Excited States: The Zincbacteriochlorin−Bacteriochlorin and Bacteriochlorophyll−Spheroidene Complexes. *J. Am. Chem. Soc.* **2004**, *126*, 4007−4016.
(81) Lange, A. W.; Herbert, J. M. Both Intra- and Interstrand Charge-Transfer Excited States in Aqueous B-DNA Are Present at Energies Comparable To, or Just Above, the $^1\pi\pi^*$ Excitonic Bright States. *J. Am. Chem. Soc.* **2009**, *131*, 3913−3922.
(82) Yamazaki, S.; Taketsugu, T. Photoreaction Channels of the Guanine−Cytosine Base Pair Explored by Long-Range Corrected TDDFT Calculations. *Phys. Chem. Chem. Phys.* **2012**, *14*, 8866−8877.
(83) Martin, R. L. Natural Transition Orbitals. *J. Chem. Phys.* **2003**, *118*, 4775−4777.